JPET Fast Forward. Published on June 7, 2024 as DOI: 10.1124/jpet.124.002120
This article has not been copyedited and formatted. The final version may differ from this version.

TITLE PAGE

Pan AMPK Activation Protects Tubules in Rat Ischemic Acute Kidney Injury [1]

Henriette Frikke-Schmidt[1], Kamal Albarazanji [1], Jenson Qi [1], David Frederick [1], Janos Steffen [1], Shanker Kalyana-Sundaram [1], Rong Meng [1], Zheng Huang Devine [1], Tao Chen[2], Qiu Li [1], Fuyong Du [1], George Ho [1], Jianying Liu [1], Roseann Riley[3], Romer A. Gonzalez-Villalobos [1], Raul C. Camacho [1], Andrea R. Nawrocki [1], Meghan Pryor[4], Min Lee[4], Victoria Wong[4], Rosalie Matico[4], Elsie Diaz[4], Daniel Krosky[4], Mark Wall[5], Elise Gao[5], Akshay A. Shah[5], James Leonard [1], Mark Erion [1], Alessandro Pocai [1], and Mark R. Player[5]

[1]Cardiovascular Metabolism, Retina and Pulmonary Hypertension, Janssen R&D, Spring House, Pennsylvania, USA; [2]Preclincial Sciences and Translational Safety, Janssen R&D, Shanghai, China; [3]Non-Clinical Safety Pathology, Janssen R&D, Spring House, Pennsylvania, USA; [4]Therapeutics Discovery, Spring House, Pennsylvania, USA; [5]Discovery Chemistry, Janssen R&D, Spring House,

This work was fully funded by Janssen Research and Development, LLC.

JPET Fast Forward. Published on June 7, 2024 as DOI: 10.1124/jpet.124.002120
This article has not been copyedited and formatted. The final version may differ from this version.

RUNNING TITLE PAGE

AMPK activation in rat AKI

24 manuscript pages

8 figures

0 tables

abstract 204 words

introduction 615 words

discussion 902 words

Corresponding author:

Henriette Frikke-Schmidt

Janssen R&D, 1400 McKean Road, Spring House, PA-19477, USA

Phone: (215) 628-5000

email: hfrikkes@its.jnj.com

Non-standard abbreviations:

ACC = Acetyl CoA Carboxylase; ADaM = allosteric drug and metabolite ; AICAR = 5-aminoimidazole-4-carboxamide ribonucleotide; AKI = Acute Kidney Injury ; AMPK = 5' adenosine monophosphate-activated protein kinase; ATN = Acute Tubular Necrosis; BUN = Blood Urea Nitrogen; CKD = Chronic Kidney Disease; ESRD = End Stage Renal Disease; ETC = Electron Transport Chain; FENa = Fractional Excretion of Sodium; FFAR4 = Free Fatty Acid Receptor 4; GFR = Glomerular Filtration Rate; GPNMB = glycoprotein (transmembrane) nmb; RPETC = renal proximal epithelial tubular cells; TGF = TubuloGlomerular Feedback

Section assignment:

Cardiovascular

JPET Fast Forward. Published on June 7, 2024 as DOI: 10.1124/jpet.124.002120
This article has not been copyedited and formatted. The final version may differ from this version.

JPET Fast Forward. Published on June 7, 2024 as DOI: 10.1124/jpet.124.002120
This article has not been copyedited and formatted. The final version may differ from this version.

ABSTRACT

Acute Kidney Injury (AKI) is characterized by an abrupt decline in kidney function and has been associated with excess risks of death, kidney disease progression, and cardiovascular events. The kidney has a high energetic demand with mitochondrial health being essential to renal function and damaged mitochondria have been reported across AKI subtypes. 5' adenosine monophosphate-activated protein kinase (AMPK) activation preserves cellular energetics through improvement of mitochondrial function and biogenesis when ATP levels are low such as under ischemia-induced AKI. We developed a selective potent small molecule pan AMPK activator, compound **1**, and tested its ability to increase AMPK activity and preserve kidney function during ischemia/reperfusion injury in rats. A single administration of Compound **1** caused sustained activation of AMPK for at least 24 hours, protected against acute tubular necrosis, and reduced clinical markers of tubular injury such as NephroCheck and Fractional Excretion of Sodium (FENa). Reduction in plasma creatinine and increased Glomerular Filtration Rate (GFR) indicated preservation of kidney function. Surprisingly, we observed a strong diuretic effect of AMPK activation associated with natriuresis both with and without AKI. Our findings demonstrate that activation of AMPK leads to protection of tubular function under hypoxic/ischemic conditions which holds promise as a potential novel therapeutic approach for AKI.

SIGNIFICANCE STATEMENT

No approved pharmacological therapies currently exist for acute kidney injury. We developed Compound **1** which dose-dependently activated AMPK in the kidney and protected kidney function and tubules after ischemic renal injury in the rat. This was accompanied by natriuresis in injured as well as uninjured rats.

JPET Fast Forward. Published on June 7, 2024 as DOI: 10.1124/jpet.124.002120
This article has not been copyedited and formatted. The final version may differ from this version.

INTRODUCTION

Acute kidney injury (AKI) is a common complication in hospitalized patients, affecting over 13 million people and resulting in 1.7 million deaths each year globally (Abd ElHafeez, 2017; Lewington, 2013; Selby, 2016). With cardiac surgery it has been found that the median incidence rate to develop ischemic AKI was 27.75% (interquartile range 16.3% to 38.86%) (Corredor, 2016) defined as a sudden renal failure, clinically manifesting in a build-up of metabolic waste products in the blood and reduction of urinary output. Left unresolved AKI can lead to the development of chronic kidney disease (CKD), end-stage renal disease (ESRD) and cardiovascular complications (Makris, 2016). Despite the significant public health burden, there are currently no approved therapies to prevent or treat AKI.

AKI can result from a wide range of septic, nephrotoxic, or ischemic insults with distinct etiologies. A common pathophysiological response across the various forms of AKI is mitochondrial dysfunction (McCullough, 2016; Morrell, 2014; Ozkok, 2014; Poyan Mehr, 2018). The renal cortex maintains one of the highest densities of mitochondria in the mammalian body, owing to the huge energetic demand of maintaining electrolyte homeostasis in the blood. When mitochondrial function is compromised by toxic insult or limited nutrient supply, this can lead to structural alterations of the tubular epithelial cells, immune cell infiltration, and ultimately apoptotic and necrotic cell death (Basile, 2012). Accordingly, there is great interest in therapeutic targets that can preserve or restore the functional capacity of mitochondria in the proximal tubules to mitigate AKI (Poyan Mehr, 2018).

5’ adenosine monophosphate-activated protein kinase (AMPK) is a multi-subunit serine/threonine kinase which responds quickly to diminished cellular energy charge by directly sensing ATP depletion and AMP elevation. AMPK activation ultimately restores ATP levels by reprogramming cellular metabolism from anabolism to catabolism (Herzig, 2018). In preclinical AKI models AMPK activity is decreased in the kidney but also in the liver. This activity decrease leads to mTORC1 activation, autophagy inhibition, and the peroxidation of accumulated lipids by oxidative stress (Au-Yeung, 2023; Decuypere, 2020; Gwon, 2017). Together with intracellular iron accumulation, lipid peroxidation is a hallmark for ferroptosis, a programmed cell death pathway activated in AKI(Du, 2023). AMPK activation has shown promise in preclinical models of AKI because AMPK promotes autophagy through ULK1 phosphorylation,

JPET Fast Forward. Published on June 7, 2024 as DOI: 10.1124/jpet.124.002120
This article has not been copyedited and formatted. The final version may differ from this version.

improves mitochondrial function and, prevents lipid accumulation by activating β-oxidation and decreasing malonyl-CoA production, the endogenous inhibitor of carnitine palmitoyltransferase 1 (CPT1) (Garcia, 2017; Kim, 2011). Further AMPK activation has been reported to increase cellular glucose uptake by phosphorylating TBC domain family, member 1 (TBC1D1) to boost glycolysis and inducing the expression of hexokinase II (HK2) to ultimately restore ATP levels (Lieberthal, 2016; Wu, 2013). However, the compounds most frequently cited include AMP mimetics, such as 5-aminoimidazole-4-carboxamide ribonucleotide (AICAR) (Lempiainen, 2012; Tsogbadrakh, 2019), or mild inhibitors of OXPHOS, such as the biguanide metformin (Jin, 2020; Li, 2016). Such compounds are known to have AMPK-independent effects and exhibit pharmacokinetic properties which limit their clinical utility (Visnjic, 2021). Our pharmacological approach was to create a small molecule activator binding a unique structural motif, called the allosteric drug and metabolite (ADaM) site, formed by an interaction between the α and β subunits (Steinberg, 2019). Several potent ADaM site binders have previously been developed with the goal of promoting insulin-independent glucose uptake into skeletal muscle (Cokorinos, 2017; Myers, 2017). Importantly, AMPK activators such as MK-8722 and PF-577 have also been shown to affect the rodent kidney, lowering proteinuria and kidney injury markers in rat models of diabetic nephropathy (Salatto, 2017; Zhou, 2019). As the human kidney contains mixed expression of β1 and β2 isoforms we set out to develop a potent ADaM site-binding AMPK pan-activator and test its ability to restore kidney function in a rat ischemia/reperfusion injury (IRI) model.

MATERIALS AND METHODS

In vivo studies

Animals:

Animal studies were performed in accordance with the Federal Animal Welfare Act, and protocols were approved by the Institutional Animal Care and Use Committee at Janssen Pharmaceutical R&D (Spring House, PA).

For each study, male (200-220 g) Sprague-Dawley rats were purchased from Charles River Laboratories (Wilmington, MA). Rats were individually housed in a temperature-controlled room with a 12:12-hours

JPET Fast Forward. Published on June 7, 2024 as DOI: 10.1124/jpet.124.002120
This article has not been copyedited and formatted. The final version may differ from this version.

light-dark cycle and allowed *ad libitum* access to water and standard rat chow diet (LabDiet 5053, PMI Nutrition International LLC, MN, USA) and acclimated to the vivarium for 1 week before their use for experiments. On average rats weighed 250-290 g at the time of procedure and were randomized to similar bodyweights the day before any study.

Treatment with Compound 1 and furosemide

Rats were SC injected with vehicle (20% Hydroxypropyl-beta-cyclodextrin), Compound **1**, or furosemide (Sigma-Aldrich, St Louis, MI, USA) dissolved to give an injection volume of 5ml/kg.

Induction of in vivo ischemia/reperfusion injury (IRI)

All rats were weighed and stratified into groups based on their body weight before surgery. Rats were anesthetized with 2% isoflurane, the surgical sites were shaved and scrubbed with chlorhexidine, ophthalmic lubricating ointment were applied to the eyes to prevent drying during the procedure. Long-acting analgesic, Ethiqa XR (0.65 mg/kg), was sc injected before surgical procedure. Surgeries were performed on a water bath-heated pad at 41°C. Temperature in the surgery room maintained at 24.4°C. Both kidneys were exposed with bilateral flank incisions and ischemia induced by clamping both renal pedicles with a small nontraumatic vascular clamp (Roboz RS-5452). The clamps were released after 33-35 minutes (depending on the surgeon, clamping time differed between studies but never between groups in the same study), and tissue reperfusion was visually confirmed. The muscle layer of the incisions was closed with suture (Ethicon, coated Vicryl 5-0) followed by closure of the skin incisions with wound clips (Braintree, 9 mm-rat). All rats received 0.5mL of sterile 0.9%NaCl saline (sc) immediately post-surgery to replenish for fluid loss. Then rats transferred to post-surgery recovery cages heated on an electric heating pad (WC02 HOTDOG controller, 37°C), rats left until they are upright and mobile, then moved to their standard clean cages. Sham-operated rats underwent the same surgical procedure without renal pedicle clamping.

Metabolic cages

Rats were placed in individual metabolism cages (Lab Products, Ilc, Delaware, USA) for a total of 2 days. The first day allowed the rats to acclimate to their cage overnight with free access to water and food

JPET Fast Forward. Published on June 7, 2024 as DOI: 10.1124/jpet.124.002120
This article has not been copyedited and formatted. The final version may differ from this version.

(LabDiet, 5053 powder diet). In studies using uninjured rats the animals were placed in the metabolic cage immediately after injection. IRI rats were allowed to recover from surgery in their home cage prior to being put back in the metabolic cage for urine collection. This gave a delay of about 3 hours after the first injection (injections one hour prior to surgery, rats then spent about 45 minutes on the surgical table before being transferred to a cage in a warm room and allowed to recover for an additional hour). On the second day water and food intake as well as urine output were measured for up to 24 hours. In studies with multiple urine collections the collection tube was removed and replaced with a fresh tube.

GFR

Transcutaneous glomerular filtration rate (GFR) was assessed at 5-7 hours post treatment or at 22-24 hours post ischemia reperfusion and treatment using fluorescein–isothiocyanate–(FITC)–sinistrin clearance in conscious rats. Rats were briefly anesthetized with 2% isoflurane and had a patch on their flank right below the rib cage shaved, depilated, and washed with 2% chlorohexidine before placing a small adhesive patch with an LED-emitting optical transducer (Mannheim Pharma and Diagnostics GmbH). Baseline measurements were recorded for 3–5 minutes, thereafter a single bolus injection of FITC-sinistrin 25 mg/kg (50 mg/mL in PBS, 0.5 ml/kg) was administered via the penile vein. Rats recovered from the anesthesia in singly housed polyurethane standard cages or in singly housed metabolism cages and transcutaneous measurements of GFR were recorded for 2 hours. FITC-sinistrin disappearance kinetics were analyzed via a three-compartment model with linear fit using MPD Studio software (MediBeacon, Mannheim, Germany). The FITC-sinistrin half-life (in minutes) was converted to GFR (in µL/minute).

Blood sampling, euthanasia, and tissue harvest

Non-terminal blood sampling took place via tail snip. For all termination studies the rats were anesthetized using isoflurane and a midline incision was made and spot urine was collected from the urinary bladder. The left kidney was then decapsulated, the left renal pedicle was clamped, and the top pole of kidney was immediately removed and freeze-clamped in liquid nitrogen. Terminal blood was collected by cardiac puncture before extracting the right kidney.

JPET Fast Forward. Published on June 7, 2024 as DOI: 10.1124/jpet.124.002120
This article has not been copyedited and formatted. The final version may differ from this version.

Blood sample processing and analysis

Blood cell GPNMB

Freshly collected whole blood was added to PAXgene solution (BD Biosciences, Franklin Lakes, NJ, USA) in a 1:2 ratio. RNA was isolated following the steps according to PAXgene RNA isolation kit (Qiagen, Hilden, Germany). The purity and concentration of RNA was determined by measuring the absorbance at 260 nm and 280 nm with the NanoDrop Spectrophotometer. cDNA was synthesized using the Superscript IV VILO Reverse Transcriptase Kit (Thermo Fisher Scientific). Quantitative real-time PCR data was generated using the QuantStudio Real-time PCR System (Thermo Fisher Scientific). Cyclophilin A (PPIA) was used as a housekeeping gene, and quantification of the data was generated using the 2ΔΔCt method. The primers used were purchased from Thermo Fisher Scientific, and their catalog numbers were as follows: PPIA (Cat#Rn00690933_m1) and GPNMB (Cat#Rn00591060_m1).

Creatinine and BUN

Blood was collected in Li-Heparin tubes (BD Vacutainer), kept briefly on ice and spun down for 10 minutes at 10,000xG and 4°C. For creatinine plasma samples were mixed with 5 volumes of water containing 2.5 uM d3-creatinine (Cambridge Isotope Labs) as internal standard and then precipitated with acetonitrile. Creatinine was analyzed by monitoring 114.1/44.1 on a Sciex QTrap 5500 operated at positive electrospray mode. Levels were calculated against internal standards d3-creatinine (117.1/47.1). The analytes were separated on a Waters XBridge Amide column (2.1x50 mm, 3.5 um) at an isocratic flow at 0.35 ml/min of solvent containing 3 mM ammonium acetate and 0.03% formic acid in 70% acetonitrile.

BUN was measured by VET AXCEL Clinical Analyzer (Alfa Wassermann), using BUN tests as per manufacturer's instructions (Catalog # SA2024). Plasma samples were diluted 1:4 in dH2O before measuring.

Sodium

JPET Fast Forward. Published on June 7, 2024 as DOI: 10.1124/jpet.124.002120
This article has not been copyedited and formatted. The final version may differ from this version.

Blood was collected in Li-Heparin tubes (BD Vacutainer), kept briefly on ice and spun down for 10 minutes at 10,000xG and 4°C before plasma was transferred into MiniCollect complete Z no additive tubes (Greiner Bio-One, Monroe, North Carolina) and analyzed using the Atellica^{R} CH Analyzer (Siemens Healthineers, Munich, Germany).

Urine collection and analysis

Creatinine

Spot urine or urine collected in metabolic cages were analyzed for creatinine using LCMS as described under blood sample processing and analysis after being diluted 10fold with water prior to processing.

Sodium

Urine was collected and analyzed as described under blood sodium measurements

NephroCheck

Rat TIMP2 and IGFBP7 protein levels in the urine were measured using commercially available ELISAs (TIMP2: #LS-F2962; LSBio, Seattle, WA, USA; IGFBP7: LS-F25306; LSBio, Seattle, WA, USA) according to manufacturer's instructions. The samples were diluted 1:6 in the sample diluent before the ELISA assays.

Kidney processing and analysis

pAMPK

Freeze-clamped kidney tissue was kept at –80C until processing. Frozen tissue fragments (~60 mg) were suspended in 10X volume of T-Per protein extraction buffer supplemented with proteinase and phosphatase inhibitor tablets (ThermoFisher) and transferred to bead-containing 2 mL tubes (MP Lysing Matrix Z) on ice. Samples were homogenized twice (MP FastPrep homogenizer) with the default settings for mouse kidney tissue. Samples were then centrifuged at 18000 xg for 20min at 4˚C, diluted 1:20 in protein extraction buffer, and protein concentration was measured by BCA assay (Pierce). Lysates were normalized to 0.6 ug/uL of protein in 0.1x WES running buffer, then loaded and run on the WES

JPET Fast Forward. Published on June 7, 2024 as DOI: 10.1124/jpet.124.002120
This article has not been copyedited and formatted. The final version may differ from this version.

automated Western blot system (ProteinSimple) and analyzed using Compass software according to manufacturer instructions. Antibodies were diluted 1:12 for pAMPK (Cell Signaling 50081S), 1:50 for AMPK (Cell Signaling 5831S), and 1:15000 for GAPDH (Cell Signaling 5174S). Automated target band identification was performed with a tolerance of 6 kD for (p)AMPK (62 kD) and GAPDH (40 kD). Traditional Western blots were also run according to standard techniques using 4-20% Tris-glycine gels, the iBLOT2 transfer system (Life Technologies), the Odyssey imaging system (LI-COR), and the same antibodies as above. Target engagement was determined by the signal ratios for a given sample across respective blots: (pAMPK/GAPDH)/(AMPK/GAPDH).

RNA seq processing

Total RNA was extracted from rat kidney using Trizol reagent and RNeasy plus mini kit (Qiagen) according to the manufacturer's instructions. RNA Integrity Number (RIN) was assessed using Agilent Bioanalyzer System. RNA Libraries were prepared from 100ng of total RNA using the KAPA RNA HyperPrep Kit with RiboErase (HMR) (Roche) according to manufacturer's instruction. Sequence-ready libraries were validated and quantitated using the Agilent High Sensitivity D1000. Individual libraries were normalized to 3nM and quantified by qPCR using the KAPA Library Quantification Kit – Illumina/ROX Low (Roche) on the QuantStudio 12K Flex Real-Time PCR System (Applied Biosystems) according to manufacturer's instructions. The libraries were pooled to 2nM and quantified again by qPCR as described above. The quantified library pool was denatured and diluted according to the NovaSeq 6000 Denature and Dilute Libraries Guide and loaded onto a NovaSeq Reagent Kit v1.5 (300 cycles) for paired end sequencing using the NovaSeq 6000 System (Illumina). BCL conversion and demultiplexing was performed using the bcl2fastq2 script (v2.20, Illumina). Data analysis was performed on QIAGEN OmicSoft Studio software version 10.0.1.81. The fastq files were mapped to the reference Rattus rattus genome (Build Rat.B6.0) using Omicsoft Aligner, and the transcripts were quantified with the "Ensemble R104" gene model. Differentially regulated genes for each contrast of interest were identified using the DESeq2 package v1.22.2. All parameters for DESeq2 were set as default. False discovery rate (FDR) < 0.1 and log2 (fold change) >1 or log2 (fold change) < -1 used as a significance threshold to define the DEGs for each contrast. The up and down-regulated genes are then subjected to enrichment

JPET Fast Forward. Published on June 7, 2024 as DOI: 10.1124/jpet.124.002120
This article has not been copyedited and formatted. The final version may differ from this version.

analysis using a Benjamini–Hochberg-adjusted P value <0.05 as the significance threshold. The Ingenuity Pathway Analysis (IPA) software (www.qiagen.com/ingenuity, Spring 2019, QIAGEN, CA, USA) was used to identify enriched biological pathways. A p-value or Benjamini-Hochberg adjusted p-value was calculated using Fisher's exact test, and a cut-off value of less than 0.05 was used to identify significantly enriched canonical pathways based on the Ingenuity Knowledge Base.

Acute tubular necrosis histological evaluation

After extraction of the right kidney a 2 mm thick cross section was cut from the middle, collected into cassettes and then fixed in 10% formalin (NFB) for 48 hours, then rinsed in 70% ethanol. After being embedded in paraffin, sections were cut at a thickness of 4um and stained with hematoxylin and eosin (H&E) staining. A histological scoring system was graded on a five-level scale (0 (no injury); 1 (0–20%); 2 (21–40%); 3 (41–60%); 4 (61–80%); 5 (81–100%). The percentage of acute tubular injury (ATN) in the kidney cortex and outer medulla regions were estimated by the same histopathologist for all studies.

***In vitro* studies for pan AMPK activation**

AMPK enzymatic assays

The increase in kinase activity by small molecule allosteric pAMPK activators was measured by quantifying the amount of ADP generated during kinase reaction with two isoforms, a1β2γ1 and a2β1γ1, of human or rat AMPK complexes which were activated (Janssen R & D). The titration of activators was incubated with 1.5 nM (human a1β2γ1), 6 nM (human a2β1γ1), 0.25 nM (rat a1β2γ1), or 2 nM (rat a2β1γ1) activated AMPK and 15 μM, 10 μM, 10 μM, or 15 μM SAMS peptides (Biosynth, Staad, Switzerland; peptide sequence: HMRSAMSGLHLVKRR) respectively for 15 minutes. The kinase reaction was initiated by addition of 35 μM, 20 μM, 17 μM, or 35 μM ATP respectively. After 1 hour reaction, the amount of ADP generated was measured with ADP-Glo Kinase Assay (Promega, Madison, Wisconsin) by following the manufacturer's instructions. The kinase assay buffer was prepared with 20 mM HEPES, 4 mM $MgCl_2$, 1 mM DTT, 1 mM EDTA, 0.01 % ovalbumin, and 0.001 % Tween-20. The kinase reaction was performed on ProxiPlate-384 Plus white 384-well microplates (Perkin Elmer, Waltham, Massachusetts), and luminescence signal was read on PHERAstar FSX microplate reader

JPET Fast Forward. Published on June 7, 2024 as DOI: 10.1124/jpet.124.002120
This article has not been copyedited and formatted. The final version may differ from this version.

(BMG Labtech, Ortenberg, Germany). The data analysis and relative EC_{50} determination was performed using GeneData Screener software (GeneData, Basel, Switzerland).

HepG2 and RPTEC pACC assays

The ability of compounds to increase pAMPK activity in live cells was determined by measuring the level of phosphorylated ACC (Acetyl CoA Carboxylase), which is directly phosphorylated by activated pAMPK. HepG2 (human hepatocellular carcinoma; ATCC, Manassas, VA) were cultured and seeded at 7,500 cells per well on Poly-D-Lysine-coated 384-well cell culture microplates (Griener bio-one, Frickenhausen, Germany) in Opti-MEM (Thermo Fisher Scientific, Waltham, MA). RPTEC (human renal proximal tubule epithelial cells; Lonza, Basel, Switzerland) were cultured and seeded at 10,000 cells per well on tissue culture treated 384-well cell culture microplates in Lonza renal epithelial growth media. The cells were incubated in cell culture incubator (37°C, 5% CO_2, 95% RH) for 24 hours and treated with titration of compounds for 30 minutes. The level of phospho-ACC in the compound treated cells was measured with AlphaLISA SureFire Ultra p-ACC (Ser79) assay kit (Perkin Elmer, Waltham, MA) by following the manufacturer's instructions (2-plate, adherent cell assay method), except using 4 times higher Alpha Streptavidin Donor Beads concentration for the HepG2 samples with the assay medium that contains biotin. AlphaLISA signal from the assay plates was read on PHERAstar FSX microplate reader (BMG Labtech, Ortenberg, Germany). The data analysis and relative EC50 determination was performed using GeneData Screener software (GeneData, Basel, Switzerland).

***In vitro* studies with hypoxic injury**

Human kidney proximal tubule HK-2 cells (ATTC, CRL-2190) were grown in Keratinocytes SFM (Thermo Fisher) at 37°C, 5% CO_2. For drug treatments HK-2 cells were treated with different concentrations of Compound **1** or 0.1% DMSO as vehicle control. Hypoxic conditions were established using an AVATAR system (xcellbio) at 0.2% O_2, 5% CO_2 and 0.5psi for 48 hours.

Cell viability

JPET Fast Forward. Published on June 7, 2024 as DOI: 10.1124/jpet.124.002120
This article has not been copyedited and formatted. The final version may differ from this version.

HK-2 cells were plated in 96 well white wall plates at a density of 15000 cells/ well. After 24 hours the cells were treated with Compound **1** or DMSO and grown under normoxia or hypoxia (see above for conditions) for 48 hours. Cell viability was measured using the Cell-Titer-Glo (Promega) assay according to the manufacturer's recommendation.

Caspase 3/7 activity assay

HK-2 cells were plated in 96 well white wall plates at at density of 15000 cells/ well. After 24 hours the cells were treated with Compound **1** or DMSO and grown under normoxia or hypoxia (see above for conditions) for 48 hours. Caspase 3/7 activity was determined using the Caspase-Glo® 3/7 Assay System (Promega) according to the manufacturer's recommendation.

Mitochondrial Respiration Measurement

HK-2 cells were grown in Seahorse XF96 V3 PS Cell Culture Microplates (Agilent) at a cell density of 12500 cells/well under normoxia or hypoxia for 48 hours. Mitochondrial respiration was measured using the Seahorse XFe96 analyzer (Agilent) and the Seahorse XF Cell Mito Stress Test Kit (Agilent). During the assay 1.5µM oligomycin, 0.5µM FCCP and 0.5 µM rotenone/antimycin A were used. After the assay the cells were stained with Hoechst 33342 at 2µg/ml for 15 minutes and then counted with the Cytation 5 Cell Imaging Multimode Reader (Biotek Instruments) and the Cell Imaging software (Agilent). All respiratory data was normalized to cell count.

Mitochondrial membrane potential

HK-2 cells were plated in 96 well black wall plates at a density of 15000 cells/ well. After 24 hours the cells were treated with Compound **1** or DMSO and grown under normoxia or hypoxia (see above for conditions) for 48 hours. The mitochondrial membrane potential was analyzed with the JC-1 - Mitochondrial Membrane Potential Assay Kit (Abcam) according to the manufacturer's recommendation.

Statistical analysis

All statistical analysis used to interpret the data have been provided in the figure captions.

RESULTS

JPET Fast Forward. Published on June 7, 2024 as DOI: 10.1124/jpet.124.002120
This article has not been copyedited and formatted. The final version may differ from this version.

Compound 1 is a potent pan-AMPK activator

Our internal efforts identified a potent and pan-active AMPK activator compound **1** (see Figure 1a for structure). To confirm that **1** was a pan-activator of AMPK, recombinant heterotrimers of AMPK containing either α1β2γ1 or α2β1γ1 were reconstituted *in vitro* and tested for the ability to phosphorylate SAMS peptide (Figure 1B). **1** caused activation of the heterotrimers containing both β1 and β2 from human and rat constructs. Furthermore, we confirmed the cell penetrance of **1** by measuring the phosphorylation of Acetyl CoA Carboxylase (ACC), a well-validated AMPK substrate, in human hepatocytes (HepG2) and renal proximal tubular cells (RPTECs) (Figure 2C). HepG2 cells showed dose-responsive ACC phosphorylation, with an EC_{50} of 19.5 nM, whereas the response was right shifted in RPTECs to an EC_{50} of 98.9 nM. A significant right shift in human tubular cells was consistent across all pan-AMPK activators tested (data not shown).

Compound 1 dose-dependently activates AMPK in whole blood cells and kidney

Before testing the ability of **1** to activate AMPK in the rat kidney, we confirmed previous reports (Lempiainen, 2012) that phosphorylation of AMPK Thr172 was indeed decreased following bilateral ischemia reperfusion injury (IRI) in Spraque Dawley (SD) rats, indicating reduced AMPK activity (Figure 2A. pAMPK WES blots depicted in supplemental Figure 1A). When > 10mg/kg of **1** was administered by subcutaneous injection in uninjured, healthy rats we found significant and sustained elevation of pAMPK in kidney lysates compared to vehicle-treated animals (Figure 2B, pAMPK WES blots in supplemental figure 1). Consistently, **1** levels in plasma and kidney increased in a dose-responsive manner in these animals (Supplemental Table 1). Only the higher doses of 30 and 100 mg/kg drove AMPK activation 7 hours after administration (Figure 2C). As an additional biomarker for AMPK activation we quantified whole blood gene expression of glycoprotein (transmembrane) nmb (GPNMB) (Grempler, 2018), and found up to a 40-fold upregulation of GPNMB mRNA 7 hours after administration (Figure 2F). Under the condition of renal injury, **1** was administered to rats 1 hour before surgery, and we found that all doses significantly elevated renal pAMPK at 7 hours and the top dose of 100 mg/kg sustained this activation for up to 24 hours (Figure 2D, 2E). GPNMB expression showed a similar pattern (Figure 2G and 2H). To

JPET Fast Forward. Published on June 7, 2024 as DOI: 10.1124/jpet.124.002120
This article has not been copyedited and formatted. The final version may differ from this version.

explore whether clearance of **1** was affected by the IRI surgery, we dosed rats with or without IRI and measured plasma levels of **1** over time for up to 24 hours (Figure 2I, Supplemental Table 1). Plasma levels did not differ with injury, but kidney tissue levels were higher at the 7 hours timepoint in rats with IRI ($p=0.0017$ comparing 7 hours kidney concentration in sham versus IRI rats by unpaired t-test. See supplemental table 1). In addition, we found that plasma creatinine was decreased at 7 hours with the 100 mg/kg dose, whereas Blood Urea Nitrogen (BUN) increased at the 24-hours timepoint (Supplemental Figure 2 A-D).

Compound 1 improves kidney function and protects the tubules

We next explored the effect of Compound **1** on kidney filtration function during IRI, by measuring transcutaneous glomerular filtration rate (GFR). We ran two series of studies where we either focused on early stages of injury (7 hours after dosing) or 24 hours after reperfusion. After administering the 100 mg/kg dose, we observed an approximately 30% decrease in plasma creatinine and a trend towards decreased BUN at the 7-hour timepoint, but no sustained reductions by 24 hours (Figure 3A and 3B). Consistently, GFR indicated improved filtration between 5 and 7 hours, which was not sustained between 22 and 24 hours (Figure 3C). For both the 7 hour and the 24 hours timepoints the kidney function parameters were significantly impaired (compared to sham operated rats at 24 hours). Thus, kidney function appeared to be improved for only a portion of the time during which the AMPK complex was engaged by **1** (pAMPK graphs and blots in supplemental Figure 3).

We next assessed the tubular cell function and survival after ischemic injury, as the rationale for activating AMPK before ischemia is, in part, to sustain the energy-demanding process of reabsorption for as long as possible. We analyzed spot urine for the NephroCheck peptide signature indicating renal stress and injury, as well as the ability of the kidneys to reabsorb sodium. Compound **1** given to IRI rats reduced NephroCheck after 7 hours and 24 hours (Figure 4A). Fractional Excretion of sodium (FENa) also improved significantly at 24 hours (Figure 4B). Overall, these findings support an improved ability to maintain reabsorption in the AMPK-activated kidney after ischemic injury.

JPET Fast Forward. Published on June 7, 2024 as DOI: 10.1124/jpet.124.002120
This article has not been copyedited and formatted. The final version may differ from this version.

Histopathological evaluation of the injured kidneys confirmed that lesions occurred at the 7 hours timepoint with acute tubular necrosis (ATN) being prominent in the cortex together with tubular degeneration. At the 24 hours timepoint ATN was still present in the cortex but had also started to appear in the outer medulla together with widespread tubular degeneration (supplemental Figure 6). Compound **1** treatment delayed ATN appearance in the cortex and also caused a reduction in the outer medulla at 24 hours (Figure 5A and 5B).

In attempts to further elucidate how AMPK activation impacted the injured kidney, we performed RNAseq on bulk kidney tissues collected at 7 and 24 hours comparing IRI to uninjured kidneys with and without **1** treatment. Principal component analysis revealed a clear, time-dependent clustering of transcriptional changes that was distinct from uninjured kidneys and differed between 7 and 24 hours (supplemental figure 4-A). Kidneys treated with **1** remained within the same clusters as vehicle treated rats. Pathway analysis of differentially expressed genes revealed that IRI most significantly suppressed genes annotated to metabolic processes (False Discovery Rate (FDR) $<7*10^{-67}$) and the synthesis of metabolic cofactors (FDR $<10^{-10}$) (Supplemental Figure 4).

Viability and mitochondrial respiration in HK-2 cells are protected under hypoxia with Compound 1

To directly explore how mitochondrial function might be impacted by AMPK activation under ischemic conditions, we cultured human proximal tubule HK-2 cells for 48 hours under 0.2% O_2 in the presence of Compound **1**. Upon visual inspection, Compound **1** clearly preserved cell morphology and growth compared to the vehicle controls and dose-dependently restored viability to that of normoxic cells when using ATP content as a proxy (Figure 6A and 6B). The increased viability corresponded with a reduction in caspase 3/7-dependent apoptosis (Figure 6 C). The validity of our *in vitro* hypoxic experimental set-up was confirmed by a fourfold increase of *VEGFA* expression under hypoxia, indicating that the hypoxic stress response was activated (Figure 6D). To examine the role of mitochondrial function in this protective mechanism, oxygen consumption was measured with the Seahorse Analyzer after cells emerged 48 hours of hypoxia and 1 hour of reoxygenation. After acclimating to the hypoxic environment, HK-2 cells drastically reduced basal and maximal (FCCP-induced) respiration to about 80% of normoxic

JPET Fast Forward. Published on June 7, 2024 as DOI: 10.1124/jpet.124.002120
This article has not been copyedited and formatted. The final version may differ from this version.

levels (Figure 6E, 6F). Under the same conditions, AMPK activation by Compound **1** partly restored oxygen consumption in a dose-dependent manner but did not fully reach the level of normoxia (Figure 6E and 6F). We also observed a full dissipation of the mitochondrial membrane potential under hypoxic conditions, which was partially restored by Compound **1** (Supplemental Figure 5A), indicating preserved activity of the electron transport chain (ETC). Consistently, expression of the genes *NDUSF1*, *SDHA*, *UQRC2* and *COX4I1*, representing distinctive complexes of the ETC, was also reduced under hypoxia and dose-dependently rescued by Compound **1** (Supplemental Figure 5B). Collectively, our in vitro data suggests that Compound **1** suppresses hypoxia-induced apoptosis in proximal tubule cells by improving the efficiency of oxidative phosphorylation when oxygen is otherwise limiting for aerobic respiration.

Urine output and natriuresis are increased with compound 1 treatment in IRI

We observed that BUN levels in IRI rats treated with Compound **1** did not improve at 7 hours and showed a strong trend for being elevated at 24 hours (Figure 3B). Combined with the observation that the rats appeared less active with Compound **1** treatment led us to speculate if they were dehydrated. To evaluate whether the water balance was affected by AMPK activation, rats were dosed with 100 mg/kg of Compound **1** one hour prior to surgery and then placed in metabolic cages for urine collection after they had been allowed to recover from IRI surgery for 1 hour (giving a total of about 3 hours after injection when including the one hour pre-surgery dosing time as well as time spent during the surgical procedure). One fraction was collected for up to 7 hours post Compound **1** injection (3-7 hours) and a second fraction was collected immediately after and up to 24 hours post reperfusion (7-24 hours). We found that urine volume was significantly higher in the Compound **1**-treated rats in the first fraction, whereas very little urine was produced subsequently relative to vehicle treated sham controls (Figure 7A), suggesting a diuretic action of AMPK activation. In addition, water intake was not compensating for the urinary loss (Figure 7B). Urine analysis revealed that creatinine excretion was reduced with injury, but no difference was observed in the total amount excreted between vehicle and **1**-treated rats (Figure 7C). Nonetheless, Compound **1** caused profound natriuresis early after administration, which was reverted in the later collection fraction (Figure 7D). These observations suggest that AMPK activation elicits significant natriuresis and diuresis.

JPET Fast Forward. Published on June 7, 2024 as DOI: 10.1124/jpet.124.002120
This article has not been copyedited and formatted. The final version may differ from this version.

AMPK activation promotes diuresis in normal rats

To evaluate if the diuretic effect observed in rats with IRI impact kidney functional parameters, normal rats were treated with the positive control furosemide (100 mg/kg), or Compound **1**. AMPK activation and furosemide promoted a similar diuretic effect and caused an acute elevation of plasma creatinine and BUN. Only the elevation induced by AMPK activation persisted up to 24 hours (Figure 8B and 8C) likely due to the short half-life of furosemide in rodents (Inoue, 1987). Water intake did not compensate for the elevated urine production during this time (Figure 8D and 8E). Creatinine excretion was mildly suppressed with **1** relative to furosemide in the earlier fraction, whereas natriuresis was elevated with both treatments (Figure 8F, 8G). GFR was similarly suppressed by both treatments throughout the experiment (Figure 8H).

DISCUSSION

The kidney has a high energetic demand to maintain fluid and electrolyte balance. Mitochondrial dysfunction has been linked to acute kidney disease (AKI), prompting interest in therapeutic strategies targeting mitochondrial restoration. Previous studies using non-specific AMPK activators like AICAR or metformin demonstrated renal microstructure protection during ischemic AKI. (Decleves, 2014; Lieberthal, 2016; Ma, 2022; Seo-Mayer, 2011). Using a novel small molecule AMPK activator, we evaluated the ability of selective increase in AMPK activity to preserve kidney function during ischemia/reperfusion injury in rats.

Given that sustained AMPK activation results in pathological cardiac remodeling in rodents and non-human primates (Myers, 2017), we delivered the AMPK activator as a single preventative dose, precluding exploration of sustained AMPK activation through multiple administrations, which could otherwise have shed light on AKI to CKD transition, where mitochondrial dysfunction plays a crucial role (Szeto, 2017).

Our findings indicate that acute AMPK activation using Compound **1** somewhat preserved kidney function, as evidenced by improving GFR and plasma creatinine and consistently improving markers of

JPET Fast Forward. Published on June 7, 2024 as DOI: 10.1124/jpet.124.002120
This article has not been copyedited and formatted. The final version may differ from this version.

tubular health and reabsorption. Notably, the improvement in GFR and plasma creatinine was not immediately observed at 24 hours despite positive indicators of tubular health and renal AMPK target engagement (Figure 2). The diuretic and natriuretic effect we observed with AMPK activation is expected to impact urinary markers of reabsorption as well as GFR. As shown in Figure 8 furosemide alone could decrease GFR and it is also highly likely that the reduced concentrations of the NephroCheck markers and sodium was further impacted by the increased urine volume, contributing to their improvement. To gain a comprehensive understanding, it would be necessary to evaluate furosemide alone in an ischemia/reperfusion injury (IRI) AKI model. Surprisingly, this specific evaluation has not been attempted in existing literature, leaving furosemide's impact on NephroCheck and FENa after IRI directionally unclear. We speculate that additional treatment strategies, such as rehydration, could unveil the full benefit of improved tubular health on kidney function (Patschan, 2019).

The diuretic effect observed with AMPK activation prompts speculation. From an energy preservation perspective, reducing the demand on the on the Na/K-ATPase would ultimately conserve ATP. While reports demonstrate AMPK's interaction with electrolyte transporters in the kidney, the precise impact on fluid homeostasis remains uncertain (Fraser, 2007; Huang, 2010), To rule out confounding pharmacology due to off-target binding of Compound **1**, we conducted a CEREP screen assessing 77 GPCRs, ion channels, and transporters (Appendix A/supplemental material 2). As all IC50 values were above 10µM this screening did not raise any immediate concern of Compound **1** having off target effects in vivo. Additionally the diuretic effect was corroborated by other pan AMPK ADaM site binding activators (data not shown), further supporting the on-target effect mediated by AMPK activation.

In addition to its role in enhancing mitochondrial health within proximal tubular cells, AMPK activation may exert effects on the cardiorenal system through alternative mechanisms. We used GPNMB as a biomarker for activation, as previously described by Grempler (Grempler, 2018), and observed significant upregulation in whole blood. Existing reports associate GPNMB with macrophage inflammatory response polarization, particularly favoring a shift toward M2 polarization (Zhou, 2017). This anti-inflammatory response has repeatedly been linked to having a restorative impact in rodent AKI (Kundert, 2018; Meng, 2015) and we cannot exclude that this secondary effect has affected our outcome. Several studies have

also explored how AMPK and the renin/angiotensin/vasopressin system are interdependent (Liu, 2019; Tain, 2018) and that the AMPK activator and ADaM site binder A769662 acted as a potent vasodilator in renal arteries from both rat and man (Rodriguez, 2020).

From an intracellular perspective there are plenty of pathways impacted by AMPK that have been shown to play a role in AKI as well. Renal tubular cells exposed to experimental ischemia reperfusion in vitro were found to have a protective autophagy response that could be repressed by silencing AMPK expression (Wang, 2013) further supported by the finding that preconditioning of metabolically stressed proximal tubular cells with either AICAR or A769662 protected these cells from apoptosis (Lieberthal, 2016). This response appears to be mediated by suppression of the mTOR pathway *in vitro* as well as *in vivo* (Wang, 2013; Zhou, 2023). Upstream of AMPK, Free Fatty Acid Receptor 4 (FFAR4) has been shown to be downregulated in various forms of AKI in mice and aggravate injury when genetically deleted (Yang, 2022). Interestingly, pharmacological stimulation of this receptor in cisplatin treated tubular cells caused an upregulation of pAMPK (Yang, 2022) which is further supported by the remarkable protection of renal injury by ω-3 polyunsaturated fatty acids, which are known to mediate their effect through FFAR4 (Gwon, 2017). Other studies link the protective effect of AMPK activation in AKI with reduced oxidative stress. Evidence for this comes from the observation that the antioxidant cyanidin-3-glucoside can protect against AKI by reducing ferroptosis – unless AMPK is inhibited by compound C (Du, 2023) and has even been linked to hepatic lipid accumulation taking place with AKI (Au-Yeung, 2023).

In summary, our study revealed that acute AMPK activation had a protective effect on kidney function during ischemic AKI and conferred some tubular health advantages that could extend to other AKI causes. Investigating AMPK activation in alternative rodent AKI models—such as cytotoxic or sepsis-induced injury—may shed light on the therapeutic potential of ADaM site binder-mediated AMPK activation in those scenarios. Additionally, exploring isotype-selective AMPK activators devoid of cardiac risks could facilitate further research into AMPK's role in the transition from AKI to CKD.

ACKNOWLEDGEMENTS

The authors would like to thank the staff in the vivarium at the Janssen R&D site.

DATA AVAILABILITY STATEMENT

The authors declare that all the data supporting the findings of this study are available within the paper and its Supplemental Data.

AUTHORSHIP CONTRIBUTIONS

Participated in research design: Frikke-Schmidt, Albarazanji, Qi, Frederick, Steffen, Kalyana-Sundaram, Gonzales-Villalobos, Nawrocki, Pryor, and Leonard

Conducted experiments: Frikke-Schmidt, Albarazanji, Qi, Frederick, Steffen, Devine, Li, Du, Liu, and Lee

Contributed new reagents or analytic tools: Kalyana-Sundaram, Meng, Chen, Ho, Riley, Wong, Matico, Diaz, Krosky, Wall, Gao, Shah, and Player.

Performed data analysis: Frikke-Schmidt, Frederick, Steffen, Kalyana-Sundaram, and Pryor.

Wrote or contributed to the writing of the manuscript: Frikke-Schmidt, Albarazanji, Qi, Frederick, Steffen, Chen, Gonzales-Villalobos, Camacho, Leonard, Erion, Pocai, and Player.

REFERENCES

Abd ElHafeez S, Tripepi G, Quinn R, Naga Y, Abdelmonem S, AbdelHady M, Liu P, James M, Zoccali C, Ravani P (2017) Risk, Predictors, and Outcomes of Acute Kidney Injury in Patients Admitted to Intensive Care Units in Egypt. Sci Rep 7: 17163.

Au-Yeung KKW, Shang Y, Wijerathne CUB, Madduma Hewage S, Siow YL, O K (2023) Acute Kidney Injury Induces Oxidative Stress and Hepatic Lipid Accumulation through AMPK Signaling Pathway. Antioxidants (Basel) 12:

Basile DP, Anderson MD, Sutton TA (2012) Pathophysiology of acute kidney injury. Compr Physiol 2: 1303-1353.

Cokorinos EC, Delmore J, Reyes AR, Albuquerque B, Kjobsted R, Jorgensen NO, Tran JL, Jatkar A, Cialdea K, Esquejo RM, Meissen J, Calabrese MF, Cordes J, Moccia R, Tess D, Salatto CT, Coskran TM, Opsahl AC, Flynn D, Blatnik M, Li W, Kindt E, Foretz M, Viollet B, Ward J, Kurumbail RG, Kalgutkar AS, Wojtaszewski JFP, Cameron KO, Miller RA (2017) Activation of Skeletal Muscle AMPK Promotes Glucose Disposal and Glucose Lowering in Non-human Primates and Mice. Cell Metab 25: 1147-1159 e1110.

Corredor C, Thomson R, Al-Subaie N (2016) Long-Term Consequences of Acute Kidney Injury After Cardiac Surgery: A Systematic Review and Meta-Analysis. J Cardiothorac Vasc Anesth 30: 69-75.

Decleves AE, Sharma K, Satriano J (2014) Beneficial Effects of AMP-Activated Protein Kinase Agonists in Kidney Ischemia-Reperfusion: Autophagy and Cellular Stress Markers. Nephron Exp Nephrol

Decuypere JP, Hutchinson S, Monbaliu D, Martinet W, Pirenne J, Jochmans I (2020) Autophagy Dynamics and Modulation in a Rat Model of Renal Ischemia-Reperfusion Injury. Int J Mol Sci 21:

Du YW, Li XK, Wang TT, Zhou L, Li HR, Feng L, Ma H, Liu HB (2023) Cyanidin-3-glucoside inhibits ferroptosis in renal tubular cells after ischemia/reperfusion injury via the AMPK pathway. Mol Med 29: 42.

Fraser SA, Gimenez I, Cook N, Jennings I, Katerelos M, Katsis F, Levidiotis V, Kemp BE, Power DA (2007) Regulation of the renal-specific Na+-K+-2Cl- co-transporter NKCC2 by AMP-activated protein kinase (AMPK). Biochem J 405: 85-93.

Garcia D, Shaw RJ (2017) AMPK: Mechanisms of Cellular Energy Sensing and Restoration of Metabolic Balance. Mol Cell 66: 789-800.

Grempler R, Wolff M, Simon E, Schmid R, Eisele C, Rieber K, Fischer E, Mettel S, Gabrielyan O, Delic D, Luippold G, Redeman N (2018) Discovery and translation of a target engagement marker for AMP-activated protein kinase (AMPK). PLoS One 13: e0197849.

Gwon DH, Hwang TW, Ro JY, Kang YJ, Jeong JY, Kim DK, Lim K, Kim DW, Choi DE, Kim JJ (2017) High Endogenous Accumulation of omega-3 Polyunsaturated Fatty Acids Protect against Ischemia-Reperfusion Renal Injury through AMPK-Mediated Autophagy in Fat-1 Mice. Int J Mol Sci 18:

Herzig S, Shaw RJ (2018) AMPK: guardian of metabolism and mitochondrial homeostasis. Nat Rev Mol Cell Biol 19: 121-135.

Huang DY, Gao H, Boini KM, Osswald H, Nurnberg B, Lang F (2010) In vivo stimulation of AMP-activated protein kinase enhanced tubuloglomerular feedback but reduced tubular sodium transport during high dietary NaCl intake. Pflugers Arch 460: 187-196.

Inoue M, Okajima K, Itoh K, Ando Y, Watanabe N, Yasaka T, Nagase S, Morino Y (1987) Mechanism of furosemide resistance in analbuminemic rats and hypoalbuminemic patients. Kidney Int 32: 198-203.

Jin K, Ma Y, Manrique-Caballero CL, Li H, Emlet DR, Li S, Baty CJ, Wen X, Kim-Campbell N, Frank A, Menchikova EV, Pastor-Soler NM, Hallows KR, Jackson EK, Shiva S, Pinsky MR, Zuckerbraun BS, Kellum JA, Gomez H (2020) Activation of AMP-activated protein kinase during sepsis/inflammation improves survival by preserving cellular metabolic fitness. FASEB J 34: 7036-7057.

Kim J, Kundu M, Viollet B, Guan KL (2011) AMPK and mTOR regulate autophagy through direct phosphorylation of Ulk1. Nat Cell Biol 13: 132-141.

Kundert F, Platen L, Iwakura T, Zhao Z, Marschner JA, Anders HJ (2018) Immune mechanisms in the different phases of acute tubular necrosis. Kidney Res Clin Pract 37: 185-196.

Lempiainen J, Finckenberg P, Levijoki J, Mervaala E (2012) AMPK activator AICAR ameliorates ischaemia reperfusion injury in the rat kidney. Br J Pharmacol 166: 1905-1915.

Lewington AJ, Cerda J, Mehta RL (2013) Raising awareness of acute kidney injury: a global perspective of a silent killer. Kidney Int 84: 457-467.

Li J, Gui Y, Ren J, Liu X, Feng Y, Zeng Z, He W, Yang J, Dai C (2016) Metformin Protects Against Cisplatin-Induced Tubular Cell Apoptosis and Acute Kidney Injury via AMPKalpha-regulated Autophagy Induction. Sci Rep 6: 23975.

Lieberthal W, Tang M, Lusco M, Abate M, Levine JS (2016) Preconditioning mice with activators of AMPK ameliorates ischemic acute kidney injury in vivo. Am J Physiol Renal Physiol 311: F731-F739.

Liu J, Li X, Lu Q, Ren D, Sun X, Rousselle T, Li J, Leng J (2019) AMPK: a balancer of the renin-angiotensin system. Biosci Rep 39:

Ma H, Guo X, Cui S, Wu Y, Zhang Y, Shen X, Xie C, Li J (2022) Dephosphorylation of AMP-activated protein kinase exacerbates ischemia/reperfusion-induced acute kidney injury via mitochondrial dysfunction. Kidney Int 101: 315-330.

Makris K, Spanou L (2016) Acute Kidney Injury: Definition, Pathophysiology and Clinical Phenotypes. Clin Biochem Rev 37: 85-98.

McCullough PA, Choi JP, Feghali GA, Schussler JM, Stoler RM, Vallabahn RC, Mehta A (2016) Contrast-Induced Acute Kidney Injury. J Am Coll Cardiol 68: 1465-1473.

Meng XM, Tang PM, Li J, Lan HY (2015) Macrophage Phenotype in Kidney Injury and Repair. Kidney Dis (Basel) 1: 138-146.

Morrell ED, Kellum JA, Pastor-Soler NM, Hallows KR (2014) Septic acute kidney injury: molecular mechanisms and the importance of stratification and targeting therapy. Crit Care 18: 501.

Myers RW, Guan HP, Ehrhart J, Petrov A, Prahalada S, Tozzo E, Yang X, Kurtz MM, Trujillo M, Gonzalez Trotter D, Feng D, Xu S, Eiermann G, Holahan MA, Rubins D, Conarello S, Niu X, Souza SC, Miller C, Liu J, Lu K, Feng W, Li Y, Painter RE, Milligan JA, He H, Liu F, Ogawa A, Wisniewski D, Rohm RJ, Wang L, Bunzel M, Qian Y, Zhu W, Wang H, Bennet B, LaFranco Scheuch L, Fernandez GE, Li C, Klimas M, Zhou G, van Heek M, Biftu T, Weber A, Kelley DE, Thornberry N, Erion MD, Kemp DM, Sebhat IK (2017) Systemic pan-AMPK activator MK-8722 improves glucose homeostasis but induces cardiac hypertrophy. Science 357: 507-511.

Ozkok A, Edelstein CL (2014) Pathophysiology of cisplatin-induced acute kidney injury. Biomed Res Int 2014: 967826.

Poyan Mehr A, Tran MT, Ralto KM, Leaf DE, Washco V, Messmer J, Lerner A, Kher A, Kim SH, Khoury CC, Herzig SJ, Trovato ME, Simon-Tillaux N, Lynch MR, Thadhani RI, Clish CB, Khabbaz KR, Rhee EP, Waikar SS, Berg AH, Parikh SM (2018) De novo NAD(+) biosynthetic impairment in acute kidney injury in humans. Nat Med 24: 1351-1359.

Salatto CT, Miller RA, Cameron KO, Cokorinos E, Reyes A, Ward J, Calabrese MF, Kurumbail RG, Rajamohan F, Kalgutkar AS, Tess DA, Shavnya A, Genung NE, Edmonds DJ, Jatkar A, Maciejewski BS, Amaro M, Gandhok H, Monetti M, Cialdea K, Bollinger E, Kreeger JM, Coskran TM, Opsahl AC, Boucher GG, Birnbaum MJ, DaSilva-Jardine P, Rolph T (2017) Selective Activation of AMPK beta1-Containing Isoforms Improves Kidney Function in a Rat Model of Diabetic Nephropathy. J Pharmacol Exp Ther 361: 303-311.

Selby NM, Fluck RJ, Kolhe NV, Taal MW (2016) International Criteria for Acute Kidney Injury: Advantages and Remaining Challenges. PLoS Med 13: e1002122.

Seo-Mayer PW, Thulin G, Zhang L, Alves DS, Ardito T, Kashgarian M, Caplan MJ (2011) Preactivation of AMPK by metformin may ameliorate the epithelial cell damage caused by renal ischemia. Am J Physiol Renal Physiol 301: F1346-1357.

Steinberg GR, Carling D (2019) AMP-activated protein kinase: the current landscape for drug development. Nat Rev Drug Discov 18: 527-551.

Szeto HH, Liu S, Soong Y, Seshan SV, Cohen-Gould L, Manichev V, Feldman LC, Gustafsson T (2017) Mitochondria Protection after Acute Ischemia Prevents Prolonged Upregulation of IL-1beta and IL-18 and Arrests CKD. J Am Soc Nephrol 28: 1437-1449.

Tain YL, Hsu CN (2018) AMP-Activated Protein Kinase as a Reprogramming Strategy for Hypertension and Kidney Disease of Developmental Origin. Int J Mol Sci 19:

Tsogbadrakh B, Ryu H, Ju KD, Lee J, Yun S, Yu KS, Kim HJ, Ahn C, Oh KH (2019) AICAR, an AMPK activator, protects against cisplatin-induced acute kidney injury through the JAK/STAT/SOCS pathway. Biochem Biophys Res Commun 509: 680-686.

Visnjic D, Lalic H, Dembitz V, Tomic B, Smoljo T (2021) AICAr, a Widely Used AMPK Activator with Important AMPK-Independent Effects: A Systematic Review. Cells 10:

Wang LT, Chen BL, Wu CT, Huang KH, Chiang CK, Hwa Liu S (2013) Protective role of AMP-activated protein kinase-evoked autophagy on an in vitro model of ischemia/reperfusion-induced renal tubular cell injury. PLoS One 8: e79814.

Wu N, Zheng B, Shaywitz A, Dagon Y, Tower C, Bellinger G, Shen CH, Wen J, Asara J, McGraw TE, Kahn BB, Cantley LC (2013) AMPK-dependent degradation of TXNIP upon energy stress leads to enhanced glucose uptake via GLUT1. Mol Cell 49: 1167-1175.

Yang L, Wang B, Guo F, Huang R, Liang Y, Li L, Tao S, Yin T, Fu P, Ma L (2022) FFAR4 improves the senescence of tubular epithelial cells by AMPK/SirT3 signaling in acute kidney injury. Signal Transduct Target Ther 7: 384.

Zhou BY, Yang J, Luo RR, Sun YL, Zhang HT, Yang AX, Zhang GX (2023) Dexmedetomidine Alleviates Ischemia/Reperfusion-Associated Acute Kidney Injury by Enhancing Autophagic Activity via the alpha2-AR/AMPK/mTOR Pathway. Front Biosci (Landmark Ed) 28: 323.

Zhou L, Zhuo H, Ouyang H, Liu Y, Yuan F, Sun L, Liu F, Liu H (2017) Glycoprotein non-metastatic melanoma protein b (Gpnmb) is highly expressed in macrophages of acute injured kidney and promotes M2 macrophages polarization. Cell Immunol 316: 53-60.

Zhou X, Muise ES, Haimbach R, Sebhat IK, Zhu Y, Liu F, Souza SC, Kan Y, Pinto S, Kelley DE, Hoek M (2019) PAN-AMPK Activation Improves Renal Function in a Rat Model of Progressive Diabetic Nephropathy. J Pharmacol Exp Ther 371: 45-55.

FOOTNOTES

Funding footnotes and financial disclosure

This work was fully funded by Janssen Research and Development, LLC. Competing interests: All authors are, or were, employees of Janssen R&D and may own shares of Johnson & Johnson stock.

Previous presentations of work

Parts of the work described in the current manuscript has been submitted as an abstract (but not presented) at the 2023 American Society for Nephrology (ASN) meeting. Frikke-Schmidt H, Albarazanji K, Qi J, Frederick D, Du F, Meng R, Ho G, Nawrocki AR, and Pocai A. AMPK Activation Protects Kidney Function After Renal Ischemia Reperfusion Injury in Rats. ASN. 2023.

Reprint requests

Please contact Henriette Frikke-Schmidt, Janssen R&D, 1400 McKean Road, Spring House, PA-19477, USA. Email: hfrikkes@its.jnj.com

Author affiliations in order of appearance

[1]Cardiovascular Metabolism, Retina and Pulmonary Hypertension, Janssen R&D, Spring House, Pennsylvania, USA

[2]Preclincial Sciences and Translational Safety, Janssen R&D, Shanghai, China

[3]Non-Clinical Safety Pathology, Janssen R&D, Spring House, Pennsylvania, USA

[4]Therapeutics Discovery, Spring House, Pennsylvania, USA; [5]Discovery Chemistry, Janssen R&D, Spring House

FIGURE CAPTIONS

Figure 1: Compound 1 activates all isoforms of AMP kinase

Structure of Compound **1** (A). EC_{50} values for Compound **1** activation of purified recombinant AMPK heterotrimers (B). Dose-dependent phosphorylation of ACC in HepG2s and RPTECs after 30 minutes of

JPET Fast Forward. Published on June 7, 2024 as DOI: 10.1124/jpet.124.002120
This article has not been copyedited and formatted. The final version may differ from this version.

incubation with Compound **1** (C). Data in (C) shown as mean value of 12 datapoints in HepG2 and 8 data points in RPTECs with error bars representing SEM.

Figure 2: Activation of AMPK with Compound 1 in rat kidney and whole blood.

Renal pAMPK was quantified in sham operated rats versus IRI animals (A). Compound **1** was administered to lean uninjured SD rats and AMPK activation was evaluated as either fold pAMPK over vehicle treatment at 1 hour (B) and 7 hours (C) after administration, or as whole blood GPNMB expression quantified 7 hours after administration (F). In injured rats (clamping time of 40 minutes) Compound **1** was administered by subcutaneous injection 1 hour prior to surgery and renal pAMPK was assessed at 7 hours post dosing (D) or 24 hours post reperfusion (E). Whole blood GPNMB expression was quantified from the same rats (G and H). Plasma levels of Compound **1** were measured in rats with and without IRI injury (I). In 2A: ** = $p< 0.01$ as compared to sham control (unpaired t-test). For B to H: *= $p< 0.05$; ** = $p< 0.01$, *** = $p< 0.001$ as compared to vehicle treated group (One way ANOVA followed by Dunnet's post-hoc comparison to vehicle). For I no significant differences were found when comparing the same dose in uninjured and IRI rats (mixed effects analysis followed by Tukey's multiple comparison test)

Figure 3: Effect of Compound 1 on creatinine and GFR in IRI rats

Compound **1** was administered as a single subcutaneous dose one hour before IRI in 2 separate experiments terminated at 7 hours post injection (clamping time 35 minutes) and 24 hours post reperfusion (clamping time of 33 minutes), respectively. Creatinine (figure A) and BUN (figure B) were measured from plasma samples. Transcutaneous GFR was measured from 5 to 7 hours post administration and 22-24 hours after reperfusion (figure C). *= $p< 0.05$; ** = $p< 0.01$, *** = $p< 0.001$ for difference between groups (Unpaired t-test for 7 hour data and One way ANOVA followed by Tukey's multiple comparison test for 24h data)

JPET Fast Forward. Published on June 7, 2024 as DOI: 10.1124/jpet.124.002120
This article has not been copyedited and formatted. The final version may differ from this version.

Figure 4: Urinary markers of kidney function after a single dose of Compound 1 in IRI rats

In two separate terminal studies (same animals as in figure 3), rats were given a single dose of **1** prior to surgery and spot urine and blood was collected at either 7 hours after injection or 24 hours after reperfusion. The urine was analyzed for NephroCheck (figure A), and fractional excretion of sodium (FENa) (figure B). *= $p< 0.05$; ** = $p< 0.01$, *** = $p< 0.001$ for difference between groups. Unpaired t-test for 7 hour data and One way ANOVA followed by Tukey's multiple comparison test for 24 hour data.

Figure 5: Acute tubular necrosis in rats treated with a single dose of Compound 1 one hour prior to IRI

Rats were treated with Compound **1** one hour prior to IRI surgery and kidneys were harvested either 7 hours after injection or 24 hours after perfusion (same rats as in figure 3), processed, stained for H&E before undergoing histopathological evaluation for ATN. Assessment was made in the cortex (A) and the outer strip of the outer medulla (B) where areas were scored according to the percentage of tubules being necrotic (1: <20%; 2: 21-40%; 3: 41-60%, 4: 61-80%, and 5: 81-100%). Representative images are given in figure C and D representing the cortex at 7 hours with vehicle treatment (C) and **1** treatment (D) with black arrows indicating necrotic tubules. *= $p< 0.05$; ** = $p< 0.01$ for significant difference between groups by Mann-Whitney test.

Figure 6: Compound 1 protects HK-2 cells during hypoxic conditions

HK-2 cells were treated with vehicle (DMSO) or 10µM Compound **1** and grown under hypoxic conditions for 48 hours. Shown are representative brightfield images (A). Cell viability and caspase 3/7 activity was measured in HK-2 cells that were treated with different concentrations of Compound **1** after growing for 48 hours in 0.2% oxygen. Cells in normal oxygen levels (normoxia) were only treated with

JPET Fast Forward. Published on June 7, 2024 as DOI: 10.1124/jpet.124.002120
This article has not been copyedited and formatted. The final version may differ from this version.

vehicle (DMSO) (B and C). VEGFA gene expression was quantified after hypoxic conditions (D). Mitochondrial oxygen consumption was analyzed in HK-2 cells treated as in 6B and 6C using the mitochondrial stress test (E). Basal and maximal respiration were calculated with data obtained from E (). All data presented are the mean ± SD and **p < 0.01, ***p < 0.001, ****p < 0.0001 as compared to 0µM (One-way ANOVA followed by Dunnett's post hoc comparison).

Figure 7: Urine volume and composition after injury in Compound 1-treated rats

Rats were receiving a single injection of Compound **1** one hour prior to bilateral IRI surgery (clamping time of 32 minutes). After the surgery the rats were allowed to recover before being placed in metabolic cages where urine collection took place from 3-7 hours after injection followed by collection for up to 24 hours after reperfusion. Urine production (A) and water intake (B) were quantified, and the urine was analyzed for creatinine (C) and sodium (D) content to calculate the total amounts excreted. *** = p< 0.001 for difference between groups. Mixed effects analysis followed by Sidak's multiple comparison test.

Figure 8: Urine volume and kidney function in uninjured rats after Compound 1 or furosemide

In two separate in vivo studies uninjured rats were given a single subcutaneous injection of either vehicle, 100mg/kg Compound **1** or 100mg/kg furosemide and kept in metabolic cages for either 7 hours or 24 hours. BUN and plasma creatinine were measured (B and C) and the ratio was calculated as an indication for dehydration (A). Water intake (D) and urine production (E) were quantified. Concentrations of creatinine and sodium were analyzed and used to calculate total amount of creatinine (F) and sodium (G) excreted during the collection period. GFR was measured in 2 hour window prior to termination (H). *= p< 0.05; ** = p< 0.01, *** = p< 0.001 for difference between groups (One way ANOVA followed by Tukey's multiple comparison test).

A

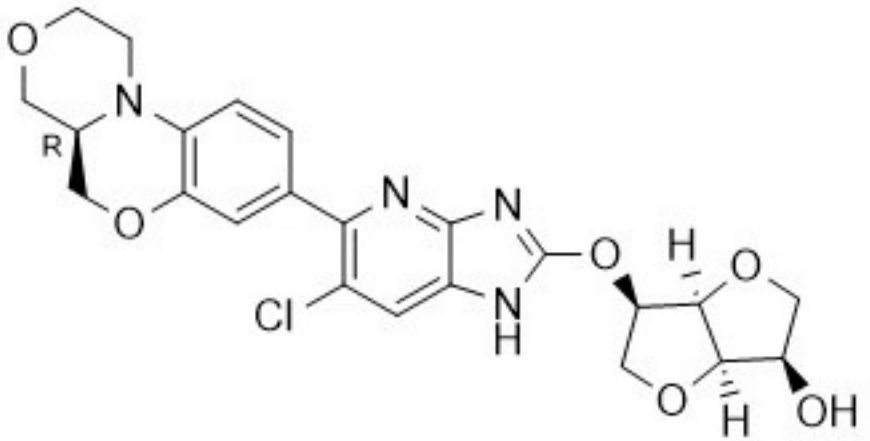

B

	EC_{50} nM	
isoform	Human	Rat
α1β2γ1	25.9	72.7
α2β1γ1	259	170

C

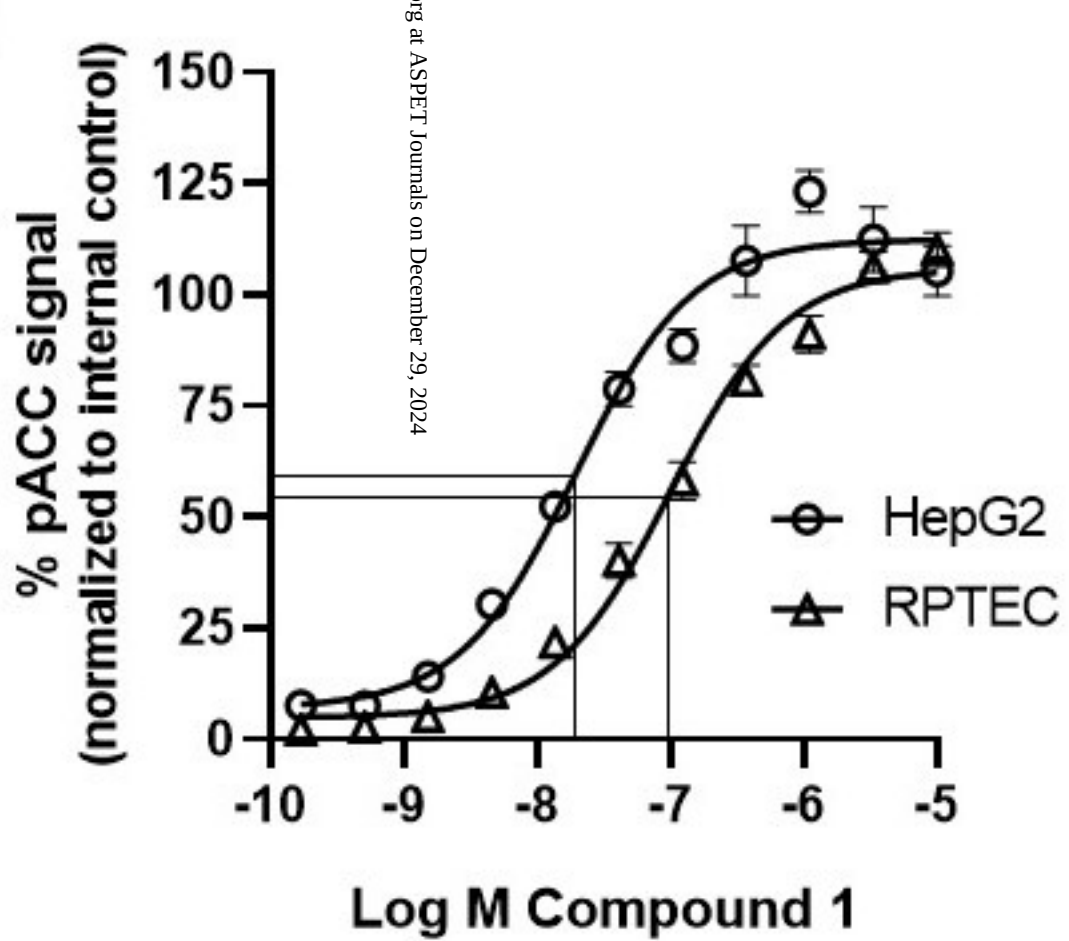

Figure 1

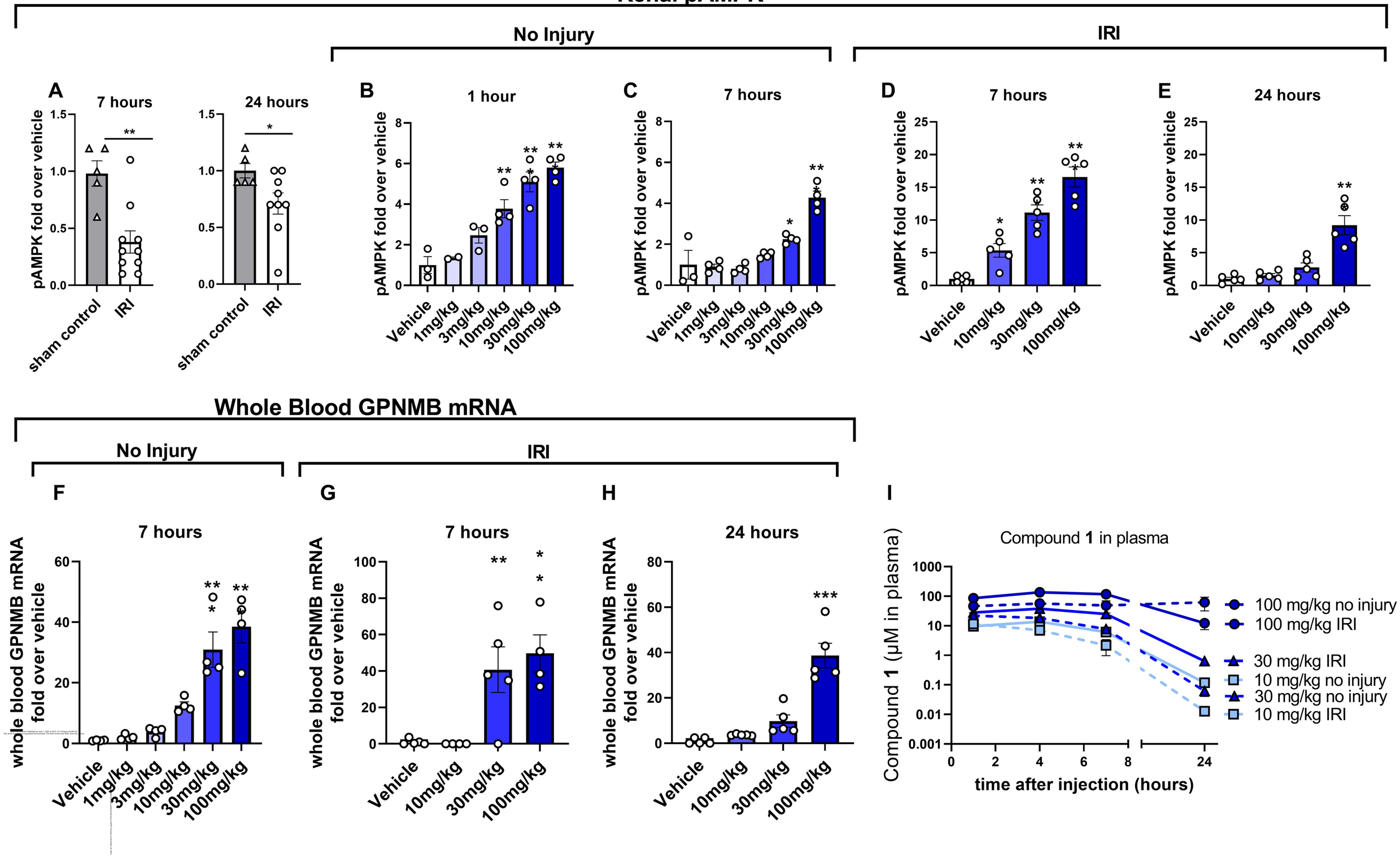
Renal pAMPK
No Injury
IRI
A
7 hours
24 hours
pAMPK fold over vehicle
sham control
IRI
B
1 hour
C
7 hours
D
7 hours
E
24 hours
Vehicle
1mg/kg
3mg/kg
10mg/kg
30mg/kg
100mg/kg
Whole Blood GPNMB mRNA
No Injury
IRI
F
7 hours
G
7 hours
H
24 hours
whole blood GPNMB mRNA fold over vehicle
I
Compound 1 in plasma
Compound 1 (µM in plasma)
time after injection (hours)
100 mg/kg no injury
100 mg/kg IRI
30 mg/kg IRI
10 mg/kg no injury
30 mg/kg no injury
10 mg/kg IRI

Figure 2

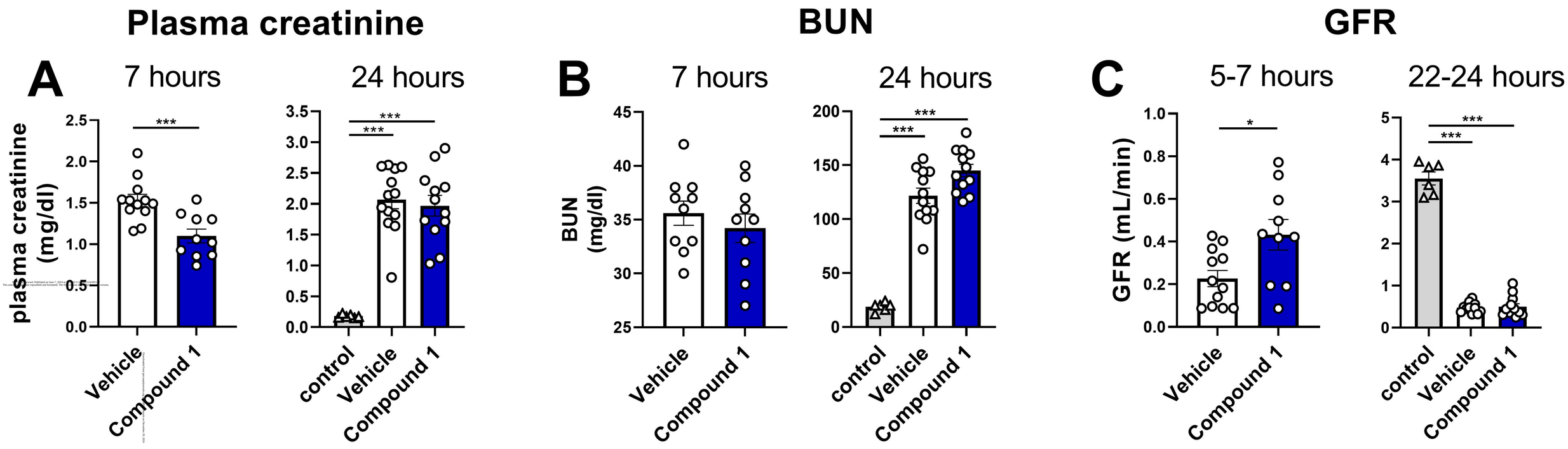
Plasma creatinine
A
7 hours
24 hours
plasma creatinine (mg/dl)
2.5
2.0
1.5
1.0
0.5
0.0
***
3.5
3.0
2.5
2.0
1.5
1.0
0.5
0.0
***
***
Vehicle
Compound 1
control
Vehicle
Compound 1
BUN
B
7 hours
24 hours
BUN (mg/dl)
45
40
35
30
25
200
150
100
50
0
***
***
Vehicle
Compound 1
control
Vehicle
Compound 1
GFR
C
5-7 hours
22-24 hours
GFR (mL/min)
1.0
0.8
0.6
0.4
0.2
0.0
*
5
4
3
2
1
0
***
***
Vehicle
Compound 1
control
Vehicle
Compound 1

Figure 3

Figure 4

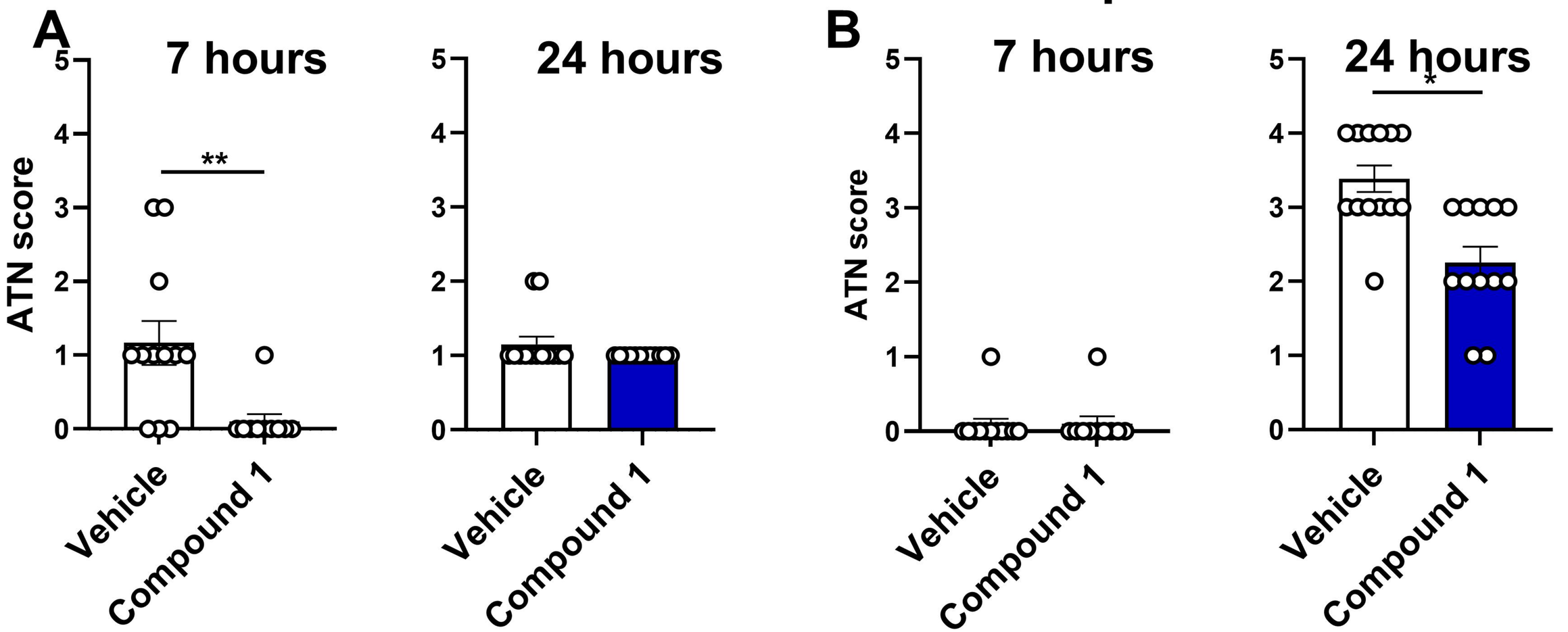

Figure 5

JPET Fast Forward. Published on June 7, 2024 as DOI: 10.1124/jpet.124.002120
This article has not been copyedited and formatted. The final version may differ from this version.

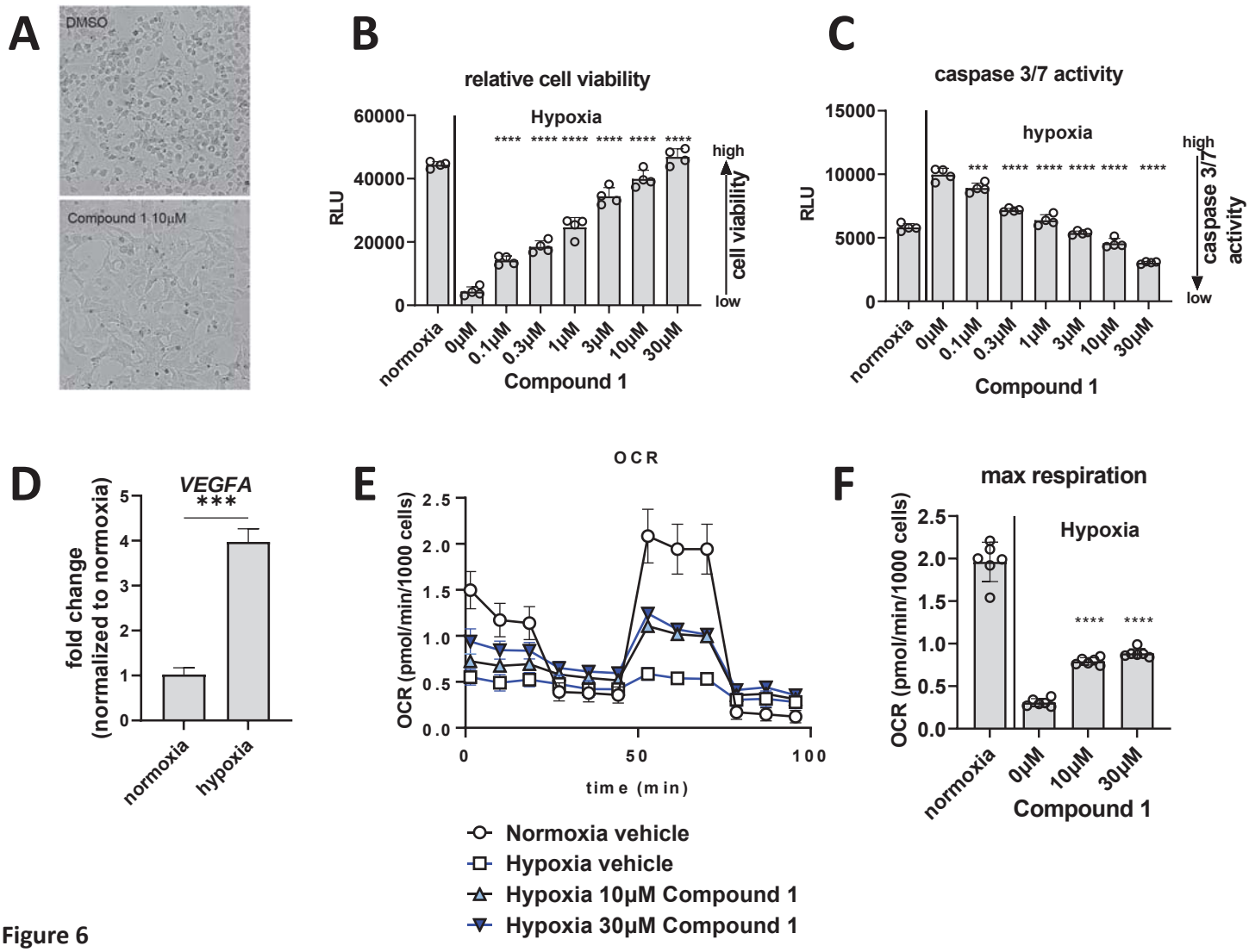

Figure 6

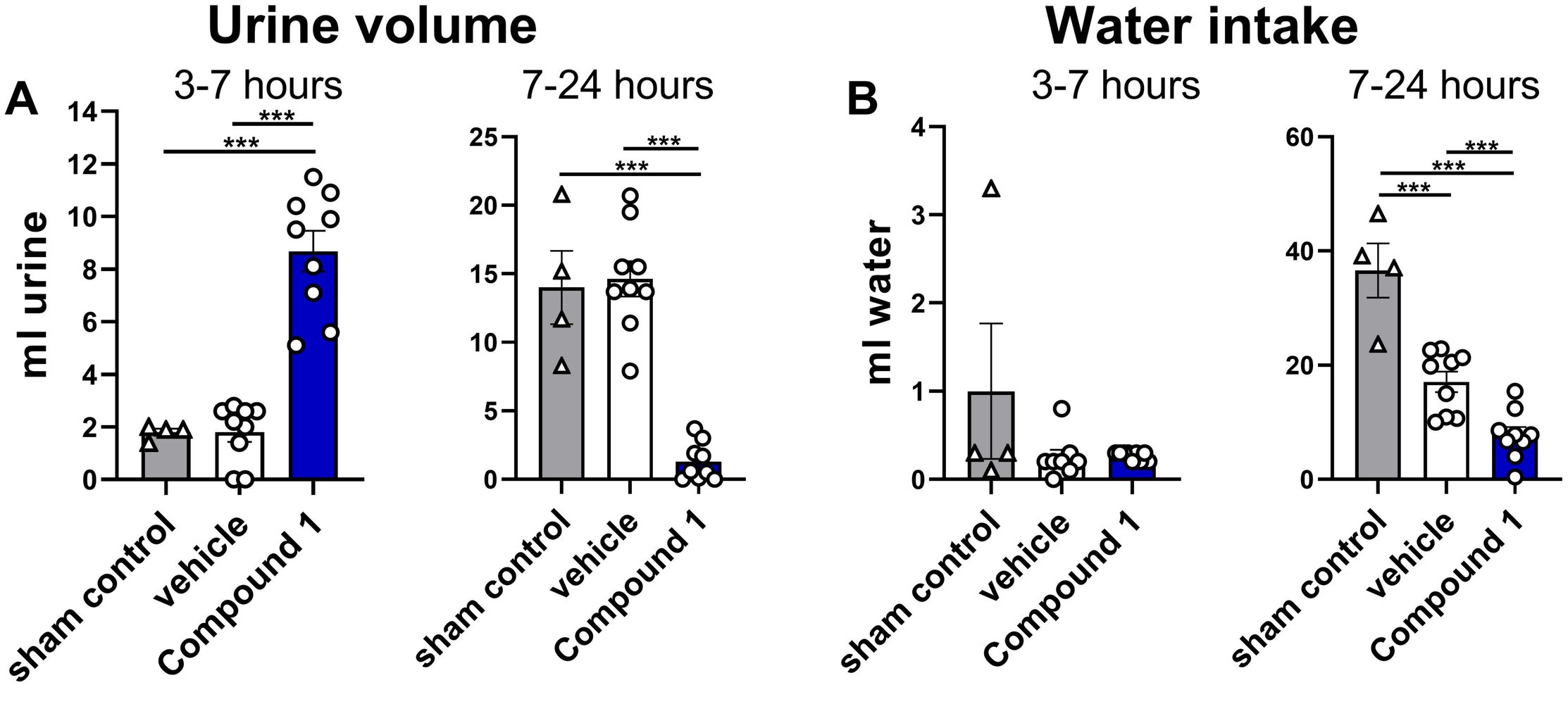
Urine volume
A
3-7 hours
7-24 hours
ml urine
***
***
***
***
sham control
vehicle
Compound 1
Water intake
B
3-7 hours
7-24 hours
ml water
***
***
***
***
sham control
vehicle
Compound 1
Creatinine excretion
C
3-7 hours
7-24 hours
mg creatinine
***
***
***
***
sham control
vehicle
Compound 1
Na excretion
D
3-7 hours
7-24 hours
mmol Na
***
***
***
***
sham control
vehicle
Compound 1

Figure 7

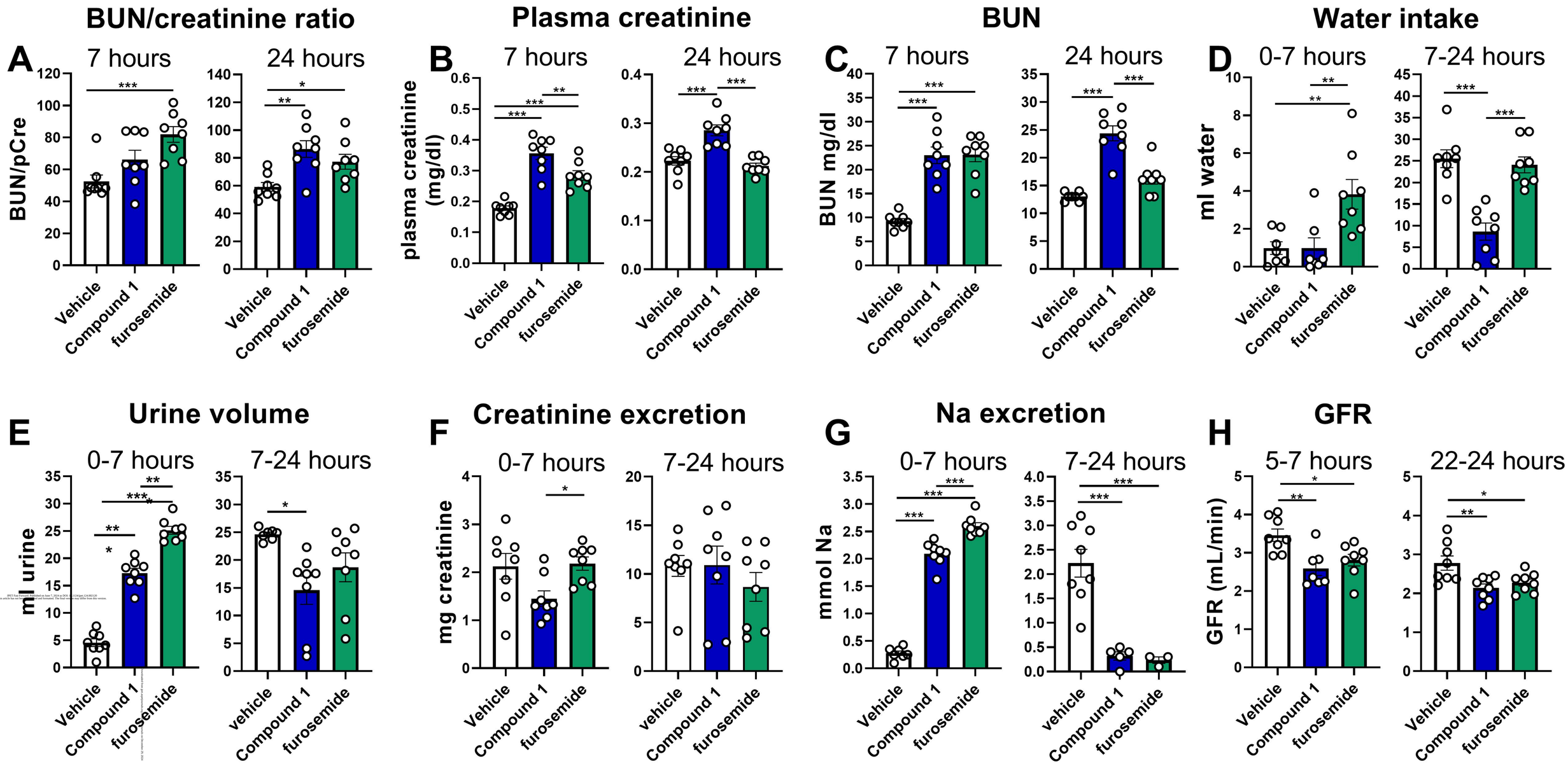
BUN/creatinine ratio
A
7 hours
24 hours
BUN/pCre
Plasma creatinine
B
7 hours
24 hours
plasma creatinine (mg/dl)
BUN
C
7 hours
24 hours
BUN mg/dl
Water intake
D
0-7 hours
7-24 hours
ml water
Urine volume
E
0-7 hours
7-24 hours
ml urine
Creatinine excretion
F
0-7 hours
7-24 hours
mg creatinine
Na excretion
G
0-7 hours
7-24 hours
mmol Na
GFR
H
5-7 hours
22-24 hours
GFR (mL/min)
Vehicle
Compound 1
furosemide
vehicle

Figure 8